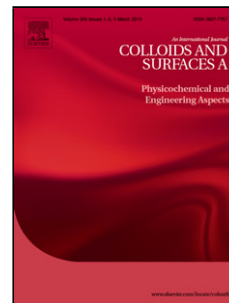# Accepted Manuscript

Title: Electrochemical properties of manganese ferrite-based supercapacitors in aqueous electrolyte: The effect of ionic radius

Author: Rongyue Wang Qun Li Lulu Cheng Hongliang Li Baoyan Wang X.S. Zhao Peizhi Guo

Please cite this article as: R. Wang, Q. Li, L. Cheng, H. Li, B. Wang, X.S. Zhao, P. Guo, Electrochemical properties of manganese ferrite-based supercapacitors in aqueous electrolyte: The effect of ionic radius, *Colloids and Surfaces A: Physicochemical and Engineering Aspects* (2014), http://dx.doi.org/10.1016/j.colsurfa.2014.05.059

Electrochemical properties of manganese ferrite-based supercapacitors in aqueous electrolyte: The effect of ionic radius

Rongyue Wang [a,b], Qun Li [a,b], Lulu Cheng [a,b], Hongliang Li [a,b], Baoyan Wang [a,b], X. S. Zhao [a,b,c], Peizhi Guo [a,b,]*

[a] Laboratory of New Fiber Materials and Modern Textile, the Growing Base for State Key Laboratory, Qingdao University, Qingdao, 266071, P. R. China

[b] School of Chemistry, Chemical Engineering and Environment, Qingdao University, Qingdao, 266071, P. R. China

[c] School of Chemical Engineering, The University of Queensland, St Lucia, QLD 4072, Australia

Corresponding author: Tel: +86 532 859 51290; Fax: +86 532 859 55529

E-mail address: guopz77@yahoo.com, pzguo@qdu.edu.cn

1

Abstract The electrochemical performances of symmetric supercapacitors assembled by $MnFe_2O_4$ colloidal nanocrystal clusters (CNCs) in aqueous electrolytes were investigated by using cyclic voltammetry, galvanostatic charge-discharge, cycle stability and electrochemical impedance spectroscopy. Results showed that the capacitance of $MnFe_2O_4$ CNCs can be easily adjusted by the controlled electrolytes. It was found that the specific capacitances of CNCs-based electrodes were 97.1, 93.9 74.2 and 47.4 F g^{-1} for the electrolytes (2 M) containing KOH, NaOH, LiOH and Na_2SO_4, respectively, at the current density of 0.1 A g^{-1}. The capacitance of the electrode was increased from 56.9 to 152.5 F g^{-1} with aqueous KOH electrolytes changed from 0.5 M to 6 M. The $MnFe_2O_4$ CNCs-based supercapacitor using aqueous KOH (6 M) electrolyte displayed the best cycle stability among all the supercapacitors. Based on the experimental results, the enhancement mechanism of electrochemical performances for the CNCs-based supercapacitors was proposed.

Keywords: $MnFe_2O_4$; Colloidal nanocrystal cluster; Supercapacitor; Electrolyte

2

1. Introduction

Nano-scale materials can show unique optical, electronic and catalytic properties compared with those bulk materials due to their small size effect and surface effect. Recently, magnetic spinel ferrites nanomaterials have received increasing interest due to their important applications, especially in energy, catalysis and biomedicine [1,2]. The synthesis and physicochemical properties of ferrite nanomaterials have been made great progress. Ferrite nanostructures with tunable sizes and morphologies including nanocrystals [3,4], hollow spheres [5], nanorods/nanowires [6] and nanotubes [7] have been successfully synthesized by using various synthetic techniques, such as hydrothermal/solvothermal method [8], thermolysis [9], template [10], sol-gel technique [11], coprecipitation [12] and electrochemical synthesis [13], etc. For example, size-tunable manganese ferrite nanocrystals can be synthesized controllably by solution phase strategies through adjusting the nature of the solvents [14-16]. MnZn ferrite nanocubes with a core-shell structure have been prepared with the assistance of mixed surfactants via a reflux method in benzyl ether systems [17].

It is well-accepted that magnetic nanocrystals with the size larger than a critical size (usually ~20 nm) show ferromagnetic behaviour [5,18]. Recently, submicrometer superparamagnetic colloidal nanocrystal clusters (CNCs) of ferrites have been synthesized based on the solvothermal method through tuning the synthetic microenvironments [5,18,19]. The superparamagnetic nature of ferrite CNCs could be ascribed to the highly-preferred orientations of the primary nanocrystals, which attributed to their excellent photocatalytic or electrocatalytic properties. $MnFe_2O_4$, as

3

a kind of spinel ferrite materials, is face-centered and cubic lattice structure. The ions of transition metal Mn and Fe which were distributed in the tetrahedral and octahedral gap, have the same intensity of ionic bonds with oxygen ion [12]. The energy storage properties of ferrites nanomaterials should be expected due to their unique composite nature and tunable-structural features.

As one type of the best energy storage devices, supercapacitor (namely electrochemical capacitor) has attracted great interest in recent years due to their excellent properties [20,21]. Compared with batteries, supercapacitors have the greater potential for providing good cyclability and high power density [22-24]. Supercapacitors mainly composed of four parts: electrode material, collector, separator and electrolyte. The synthesis of advanced electrode materials is the key issue in the development of supercapacitors. The first discovered electrode material for pseudocapacitor (one type of the supercapacitor, the other is the electric double layer capacitor) is RuO_2 [25]. Successive multielectron transfer at Ru ions, from Ru^{+4} to Ru^{+3}, then to Ru^{+2}, lead to the capacitor behaviour [26]. For the further development of affordable electrode materials, various oxide materials were investigated, such as cobalt oxide [27], nickel oxide [28] and manganese oxide [29]. Recently, ferrites have been found to exhibit good electrochemical performances either in organic Li-ion electrolyte [30] or in aqueous electrolytes [26]. In our previous reports, the effect of surfactants added into the electrolytes has been studied based on the $MnFe_2O_4$ CNCs-based supercapacitor with aqueous $LiNO_3$ electrolytes [31]. However, the electrocapacitive performances of ferrite-based electrodes still

4

need to be further clarified.

Herein, the capacitive features of $MnFe_2O_4$ CNCs-based supercapacitor have been investigated by adjusting aqueous electrolytes. Recently, we had found that $MnFe_2O_4$ colloidal nanocrystal clusters electrode displayed a higher capacitance than $MnFe_2O_4$ hollow spheres [31]. The aim of this work is to elucidate the size effect of electrolyte ions on the electrochemical properties of CNCs-based supercapacitors and the used compounds were KOH, NaOH, LiOH, Na_2SO_4 and $LiNO_3$ [31]. Furthermore, the electrocapacitive variation of the supercapacitors with the concentration of the electrolytes has been investigated. The electrochemical performances of $MnFe_2O_4$ CNCs-based supercapacitors were evaluated by cyclic voltammetry (CV), galvanostatic charge-discharge (GCD), cycle stability and electrochemical impedance spectroscopy (EIS). It is found that the capacitances of CNCs electrodes were 47.4, 51.1, 74.2, 93.9 and 97.1 F g^{-1} for the electrolytes (2 M) containing Na_2SO_4, $LiNO_3$, LiOH, NaOH and KOH, respectively, at the current density of 0.1 A g^{-1}. The capacitance of CNCs electrodes increased from 56.9 to 152.5 F g^{-1} with the KOH concentration increased from 0.5 M to 6 M at the current density of 0.1 A g^{-1}.

2. Experiments

2.1. Materials

All chemicals such as $Mn(CH_3COO)_2 \bullet 4H_2O$, $FeCl_3 \bullet 6H_2O$, CH_3COONa, KOH, NaOH, LiOH, Na_2SO_4, iso-propyl alcohol and ethylene glycol were of analytical grade and purchased from Sinopharm Chemical Reagent Company. Acetylene carbon

5

black (99.99%) and polytetrafluoroethylenelatex (PTFE 60 wt.%) were procured from Strem Chemicals and Aldrich, respectively. Double distilled water was used in all the experiments.

2.2. Synthesis of MnFe$_2$O$_4$ and Characterization

Hydrothermal method was being applied to synthesize MnFe$_2$O$_4$ CNCs. Details were described in our literature [5]. Transmission electron microscopy (TEM) images were recorded by a JEM-2000EX transmission electron microscope operated at 160 kV [5].

2.3. Electrochemical measurements

The electrodes were composed of 5 wt.% PTFE, 15 wt.% acetylene carbon black and 80 wt.% active materials. All the materials need to mix uniformity and was pressed onto a nickel foam substrate (1 cm^2) at 1.0 MPa, followed by drying in a vacuum oven at 110 ºC for 12 h. Each electrode was about 5 mg. Two electrodes were isolated by a porous membrane based on aqueous KOH (NaOH, LiOH or Na$_2$SO$_4$) electrolyte, thus form a two-electrode cell. CV, GCD, EIS and cycle stability measurements were performed by a CHI760E electrochemical workstation (CH Instrument, USA). All measurements were conducted at room temperature.

3. Results and discussions

MnFe$_2$O$_4$ CNCs were selected to investigate the effect of electrolytes on the electrochemical properties of the as-made supercapacitors because CNCs were composed of small primary nanocrystals with highly-preferred orientations. This led to a large surface area of sample CNCs that the electrolyte ions can access [31]. As

6

depicted in Fig. 1, spherical CNCs were well-dispersed with the size of about 160 nm. The unique ordered assembly of primary nanocrystals in CNCs was ascribed to its superparamagnetic behavior with an unusually large magnetization saturation value. Because of the structural feature of the materials, $MnFe_2O_4$ CNCs-based electrochemical devices have excellent superiority in the point of practical applications.

Due to the theoretical decomposition voltage of water is 1.23 V, so supercapacitors with aqueous electrolyte are supposed to be operated in voltage windows lower than 1.23 V. Hence the operating voltage higher than this will lead to the evolution of oxygen and hydrogen due to the water electrolysis. Cyclic voltammograms (CVs) of $MnFe_2O_4$ CNCs-based two-electrode supercapacitors were conducted by varying the potential window, taking the cells with aqueous 2 M KOH electrolyte as an example (Fig. 2). It can be seen that the typical capacitive behavior can be observed in a potential range of -0.2 V~1.3 V, showing an almost rectangular profile. This should be ascribed to the existence of over potential of electrode materials in pseudocapacitors, preventing the gas evolution. The electrocapacitive feature of CNCs-based supercapacitors in aqueous electrolytes should be related to the valence change at Mn-ion sites, which was close to the pseudocapacitive mechanism of manganese dioxide [5].

This paper aims to study the electrocapacitive properties of $MnFe_2O_4$ CNCs-based supercapacitors with different electrolytes. Thereafter, the voltage window in the following studies was set in the potential range of 0~1.0 V.

7

Fig. 3 shows the CV curves of CNCs-based supercapacitors with aqueous electrolytes (2 M) containing KOH, NaOH, LiOH and Na_2SO_4 at different scan rates. Clearly, the CV curves in Fig. 3A show a rectangular-like shape at 5 mV s^{-1} in the whole potential range due to a low contact resistance of the ion migration, indicating the excellent electrocapacitive features. However, the shape of the CV curves recorded at 100 mV s^{-1} was slightly tilted, as shown in Fig. 3B. This indicated that the contact resistance made the delay of the current to reach a horizontal value easy at a large scan rate, leading to a narrower loop with irregular shape [32,33]. It can be concluded from Fig. 3 that supercapacitors with the KOH electrolyte showed the largest capacitance and the capacitance of the cell containing NaOH and LiOH were larger than that using Na_2SO_4.

Fig. 4 shows the CV curves of CNCs-based supercapacitors with aqueous KOH electrolytes with the concentrations of 0.5, 2 and 6 M. It can be seen that all the CV curves of these supercapacitors displayed a rectangular shape at the scan rate of 50 mV s^{-1}. Furthermore, the areas of CV curves were gradually increased with the concentration of KOH, indicating the increase of the specific capacitance. This should be ascribed to the change of the size of hydrated K^+ ions accompanied by the variation of the concentration of the electrolytes [34,35]. With the decrease of the concentration of KOH, the total number of ions in per unit volume decreased. In the meantime, according to the formula C=Q/U, the amount of charge transported ions reduced, leading to the decrease of the capacitance. Where C is capacitance, Q is the stored charge of capacitor plate and U is the voltage between the two plates.

8

Fig. 5 refers to galvanostatic charge-discharge (GCD) curves of $MnFe_2O_4$ CNCs-based supercapacitors in aqueous electrolytes at the current densities of 0.5 A g^{-1} (A) and 2 A g^{-1} (B). All the supercapacitors showed symmetric charge-discharge curves with a small value of IR drop at the current density of 0.5 A g^{-1} (Fig. 5A), indicating the small resistance in these devices [36]. However, the IR drop increases obviously with the current density up to 2 A g^{-1} (Fig. 5B) and then these GCD curves are somewhat asymmetric compared with those in Fig. 5A. According to the equation $C_{sp}=4I\Delta t/(m\Delta E)$ the specific capacitance (C_{sp}) can be calculated [37,38]. Where I (A), Δt (s), m (g) and ΔE (V), respectively, represented the discharge current, the discharge time, the mass of active material and the potential window during the discharge process after IR drop. It can be derived that the order of the capacitance of electrode materials was the same as that obtained from the CV curves in Figs. 3 and 4. So, the $MnFe_2O_4$ electrode using the 6 M KOH electrolyte displayed the largest specific capacitance. In the meantime, the electrode materials with the 2 M Na_2SO_4 electrolyte showed the smallest capacitance. Furthermore, with the concentration of KOH increased from 0.5 M to 6 M, the capacitance was obviously increased from 35.6 to 88.7 F g^{-1}. These results indicated that the radii of hydrated ions can influence both the power (related to resistance) and energy (related to specific capacitance) performances of the supercapacitors [32].

Fig. 6 summarizes the specific capacitances of $MnFe_2O_4$ electrodes at various conditions based on the GCD curves. It can be seen that the capacitance of the electrode materials can reach as high as 152.5 F g^{-1} at the current density of 0.1 A g^{-1}

9

when using the 6 M KOH electrolyte. The capacitances of the electrodes were 97.1, 93.9, 74.2, 56.9 and 47.4 F g^{-1} for the electrolytes containing KOH (2 M), NaOH (2 M), LiOH (2 M), KOH (0.5 M) and Na$_2$SO$_4$ (2 M), respectively. Clearly, no matter what kind of electrolytes, specific capacitances of the electrode materials were decreased with the increase of the current density. On one hand, at a high current density, the electrolyte ions did not have enough time to enter inside the material, so the utilization rate of the electrode material was less, resulting in a smaller specific capacitance [33]. On the other hand, when the current density was large, the concentration polarization phenomenon was relatively obvious, thus affecting the specific capacity of supercapacitors. Compared with the capacitances of the electrode materials using the electrolytes containing KOH, NaOH, LiOH, LiNO$_3$ and Na$_2$SO$_4$ with the same concentration, the maximum specific capacitance is obtained when using the KOH electrolyte, NaOH, LiOH and LiNO$_3$ followed and Na$_2$SO$_4$ is minimal. Generally, for ions with the same charge, the smaller the radius is, the stronger polarization is in a polar solvent, leading to the stronger ionic solvation. Thereafter, the more the ions will attract the surrounding solvent molecules, thus the greater the radius of hydrated ions. The electrolyte ion transport rate thus decreased with the ion radius, reducing the capacity of the electrode material. K$^+$, Na$^+$ and Li$^+$ have the same electric charge, however, the existence of SO$_4^{2-}$ ions should further impact the energy storage at the interface due to the large size of the ions [39,40], leading to the smallest capacitance of CNCs-based electrodes in the Na$_2$SO$_4$ electrolyte. Thus the capacitances of the electrode material displayed the variation with the electrolytes

10

under the same concentration. It should also be suggested that the capacitive behavior of our $MnFe_2O_4$-based supercapacitor should be similar to those of the double layer processes due to the thick nature of the electrodes [41], which was responsible the variation of the electrochemical performances of these supercapacitors based on different electrolytes.

Electrochemical impedance spectroscopy (EIS) is a powerful tool to assess the frequency behavior and equivalent series resistance (ESR) of a supercapacitor [32]. In order to learn more about these electrodes with superior power performances, the kinetic feature of the ion diffusion in the film electrodes was investigated with a controlled manner [21]. In the present study a range of frequency from 1000 kHz to 0.01 Hz was recorded to measure the EIS spectra [42]. Fig. 7 shows the Nyquist plot of the supercapacitors with the electrolytes (2 M) containing KOH, NaOH, LiOH and Na_2SO_4 [43,44]. It can be seen from the figures that the cell showed a high frequency semicircle and a low frequency sloping line [37]. The high frequency semicircle was closely associated with the interfacial electron transfer resistance and implied that the supercapacitors had a blocking behavior [44,45]. The greater the slope of the low frequency line, the closer to the ideal supercapacitor, which means electrocapacitive behaviour [38,44]. In the equivalent circuit, R_s, known as the equivalent series resistance (ESR), refers to the electrolyte resistance, which was in accordance with the resistance of the most of the electrolyte solution and estimated from the real axis intercept at high frequency; C_{DL} reprents the electron migration resistance in the electrode; R_{ct} corresponds to the electron transfer resistance on the interface between

11

the electrode and the electrolyte; C_P corresponds to the steep line [31]. As shown in Figure 7, the magnitude of ESR of KOH is lower than that of NaOH, LiOH or Na_2SO_4, which is mainly caused by small hydrated ionic radii of K^+ ions. So, the supercapacitor assembled by aqueous KOH (2 M) electrolyte displayed the best electrochemical performance.

A simple illustration of the ions (K^+, Na^+, SO_4^{2-}, Li^+) with hydrated ionic radii was shown in Scheme 1. Removal of the outer factors, pure ionic radius is the focus of the coulomb force considering the formula $F=KQ_1Q_2/r_2$, where F is coulomb force, r is the distance between two charges (Q_1 and Q_2), K is coulomb's constant. For pure aqueous solutions, the ionic radius obey the order of r (K^+)> r (Na^+)> r (Li^+), so the coulomb force follows the rule of K^+< Na^+<Li^+. The larger coulomb force will be combined with more water molecules, making hydrated ionic radius larger. For the SO_4^{2-}, with two charges, which increase its hydrated ionic radius. For all of the above ions, specific values of hydrated ionic radii can be calculated, K^+, Na^+, SO_4^{2-} and Li^+ is 3.31 Å, 3.58 Å, 3.79 Å and 3.82 Å, respectively [46,47]. These should be responsible for the variation of electrocapacitive features with the electrolytes for these supercapacitors.

For supercapacitor, good cycle stability is very important for its practical applications [42]. Fig. 8 shows the results of the cycling performance tests of CNCs-based supercapacitors with different electrolytes by the GCD measurements at the current density of 0.25 A g^{-1}. After 2000 cycles, the capacitance retention was over 76% for the supercapacitor with the 6 M KOH electrolyte, a little higher than any of

12

the others, which indicated that the electrode material in this electrolyte had a relatively high degree of reversibility [48]. The capacitances decreased about 30% and 48% for the cells with the concentration of KOH of 2 M and 0.5 M, respectively. When using 2 M LiOH and 2 M Na_2SO_4 solutions as the electrolytes, the capacitance retention declined to 56% and 55%, respectively. These results indicated that the hydrated ionic radius as well as the charge transfer during the experiments played the key roles determining the electrochemical performances of $MnFe_2O_4$ CNCs-based supercapacitors.

4. Conclusions

The electrocapacitive properties of $MnFe_2O_4$ colloidal nanocrystal clusters (CNCs)-based supercapacitors in aqueous electrolytes have been studied. The effect of hydrated ionic radius and the electrolyte concentration were investigated based on the electrochemical characterizations of the supercapacitors. It is found that the specific capacitances of CNCs electrodes were increased with the decrease of hydrated ionic radii in alkaline electrolytes under the same conditions. The capacitance improves about 205% with the electrolytes changed from Na_2SO_4 (2 M) to KOH (2 M) solutions. Especially, the specific capacitance increased from 56.9 F g^{-1} to 152.5 F g^{-1} when the concentration of KOH changed from 0.5 M to 6 M. The electrocapacitance for the supercapacitor with the KOH (6 M) electrolyte retained about 76% of its initial value after 2000 cycles. The hydrated ionic radius in the electrolytes as well as their concentrations was suggested to play important roles in determining the electrochemical performances of ferrite-based supercapacitors.

13

References

[1]   T. Hyeon, Y. Chung, J. Park, S.S. Lee, Y.W. Kim, B.H. Park, Synthesis of highly crystalline and monodisperse cobalt ferrite nanocrystals, J. Phys. Chem. B 106 (2002) 6831-6833.

[2]   Y.M. Ren, N. Li, J. Feng, T.Z. Luan, Q. Wen, Z.S. Li, M.L. Zhang, Adsorption of Pb(II) and Cu(II) from aqueous solution on magnetic porous ferrospinel $MnFe_2O_4$, J. Colloid Interface Sci. 367 (2012) 415-421.

[3]   V.   Blanco-Gutierrez,   R.   Saez-Puche,   M.J.   Torralvo-Fernandez, Superparamagnetism and interparticle interactions in $ZnFe_2O_4$ nanocrystals, J. Mater. Chem. 22 (2012) 2992-3003.

[4]   Y. Shen, Q.D. Zhao, X.Y. Li, Y. Hou, G.H. Chen, Surface photovoltage property of magnesium ferrite/hematite heterostructured hollow nanospheres prepared with one-pot strategy, Colloids Surf. A: Physicochem. Eng. Aspects 403 (2012) 35-40.

[5]   P.Z. Guo, G.L. Zhang, J.Q. Yu, H.L. Li, X.S. Zhao, Controlled synthesis, magnetic and photocatalytic properties of hollow spheres and colloidal nanocrystal clusters of manganese ferrite, Colloids Surf A: Physicochem. Eng.

14

Aspects 395 (2012) 168-174.

[6]   J. Wang, Q.W. Chen, B.Y. Hou, Z.M. Peng, Synthesis and magnetic properties of single-crystals of MnFe$_2$O$_4$ nanorods, Eur. J. Inorg. Chem. 6 (2004) 1165-1168.

[7]   H.M. Fan, J.B. Yi, Y. Yang, K.W. Kho, H.R. Tan, Z.X. Shen, J. Ding, X.W. Sun, M.C. Olivo, Y.P. Feng, Single-crystalline MFe$_2$O$_4$ nanotubes/nanorings synthesized by thermal transformation process for biological applications, ACS Nano 3 (2009) 2798-2808.

[8]   L.J. Cui, P.Z. Guo, G.L. Zhang, Q. Li,   R.Y. Wang, M. Zhou, L.N. Ran, X.S. Zhao, Facile synthesis of cobalt ferrite submicrospheres with tunable magnetic and   electrocatalytic properties, Colloids Surf A: Physicochem. Eng. Aspects 423 (2013) 170-177.

[9]   N.Z. Bao, L.M. Shen, Y.H.A. Wang, J.X. Ma, D. Mazumdar, A. Gupta, Controlled growth of monodisperse self-supported superparamagnetic nanostructures of spherical and rod-like CoFe$_2$O$_4$ nanocrystals, J. Am. Chem. Soc. 131 (2009) 12900-12901.

[10]   Y. Xu, J. Wei, J.L. Yao, J.L. Fu, D.S. Xue, Synthesis of CoFe$_2$O$_4$ nanotube arrays through an improved sol-gel template approach, Mater. Lett. 62 (2008) 1403-1405.

[11]   S.P. Zhang, D.W. Dong, Y. Sui, Z.G. Liu, H.X. Wang, Z.N. Qian, W.H. Su, Preparation of core-shell particles consisting of cobalt ferrite and silica by sol-gel process, J. Alloys Compd. 415 (2006) 257-260.

[12]   A.J. Han, J.J. Liao, M.Q. Ye, Y. Li, X.H. Peng, Preparation of nano-MnFe$_2$O$_4$

15

and its catalytic performance of thermal decomposition of ammonium perchlorate, Chin. J. Chem. Eng. 19 (2011) 1047-1051.

[13] S.D. Sartale, C.D. Lokhande, A room temperature two-step electrochemical process for large area nanocrystalline ferrite thin films deposition, J. Electroceram. 15 (2005) 35-44.

[14] S.H. Sun, H. Zeng, D.B. Robinson, S. Raoux, P.M. Rice, S.X. Wang, G.X. Li, Monodisperse MFe_2O_4 (M = Fe, Co, Mn) nanoparticles, J. Am. Chem. Soc. 126 (2004) 273-279.

[15] J.P. Chen, C.M. Sorensen, K.J. Klabunde, G.C. Hadjipanayis, E. Devlin, A. Kostikas, Size-dependent magnetic properties of $MnFe_2O_4$ fine particles synthesized by coprecipitation, Phys. Rev. B 54 (1996) 9288-9296.

[16] M. Ghosh, G. Lawes, A. Gayen, G.N. Subbanna, W.M. Reiff, M.A. Subramanian, A.P. Ramirez, J.P. Zhang, R. Seshadri, A novel route to toluene-soluble magnetic oxide nanoparticles: aqueous hydrolysis followed by surfactant exchange, Chem. Mater. 16 (2004) 118-124.

[17] L.Y. Wang, X. Wang, J. Luo, B.N. Wanjala, C.M. Wang, N.A. Chernova, M.H. Engelhard, Y. Liu, I.T. Bae, C.J. Zhong, Core-shell structured ternary magnetic nanocubes, J. Am. Chem. Soc. 132 (2010) 17686-17689.

[18] J.P. Ge, Y.X. Hu, M. Biasini, W.P. Beyermann, Y.D. Yin, Superparamagnetic magnetite colloidal nanocrystal clusters, Angew. Chem. 46 (2007) 4342-4345.

[19] P.Z. Guo, L.J. Cui, Y.Q. Wang, M. Lv, B.Y. Wang, X.S. Zhao, Facile synthesis

16

of $ZnFe_2O_4$ nanoparticles with tunable magnetic and sensing properties, Langmuir 29 (2013) 8997-9003.

[20] P. Sena, A. Deb, Electrochemical performances of poly (3, 4-ethylenedioxythiophene)-$NiFe_2O_4$ nanocomposite as electrode for supercapacitor, Electrochim. Acta 55 (2010) 4677-4684.

[21] Z.P. Li, J.Q. Wang, Z.F. Wang, H.Q. Ran, Y. Li, X.X. Han, S.G. Yang, Synthesis of a porous birnessite manganese dioxide hierarchical structure using thermally reduced graphene oxide paper as a sacrificing template for supercapacitor application, New J. Chem. 36 (2012) 1490-1495.

[22] B.E. Conway, Transition from "supercapacitor" to "battery" behavior in electrochemical energy storage, J. Electrochem. Soc. 138 (1991) 1539-1548.

[23] B.E. Conway, V. Briss, J. Wojtowicz, The role and utilization of pseudocapacitance for energy storage by supercapacitors, J. Power Sources 66 (1997) 1-14.

[24] R. Kötz, M. Carlen, Principles and applications of electrochemical capacitors, Electrochim. Acta 45 (2000) 2483-2498.

[25] S. Trasatti, G. Buzzanca, Ruthenium dioxide: a new interesting electrode material, solid state structure and electrochemical behavior, J. Electroanal. Chem. 29 (1971) 1-2.

[26] S.L. Kuo, J.F. Lee, N.L. Wu, Study on pseudocapacitance mechanism of aqueous $MnFe_2O_4$ supercapacitor, J. Electrochem. Soc. 154 (2007) A34-A38.

[27] J. Xu, L. Gao, J. Cao, W. Wang, Z. Chen, Preparation and electrochemical

17

capacitance of cobalt oxide (Co_3O_4) nanotubes as supercapacitor material, Electrochim. Acta 56 (2010) 732-736.

[28]   Q. Lu, Z.J. Mellinger, W.G. Wang, W.F. Li, Y.P. Chen, J.G. Chen, Differentiation of bulk and surface contribution to supercapacitance in amorphous and crystalline NiO, ChemSusChem 3 (2010) 1367-1370.

[29]   C.C. Hu, T.W. Tsou, The optimization of specific capacitance of amorphous manganese oxide for electrochemical supercapacitors using experimental strategies, J. Power Sources 115 (2003) 179-182.

[30]   S.L. Kuo, N.L. Wu, Electrochemical capacitor of $MnFe_2O_4$ with organic Li-ion electrolyte, Electrochem. Solid. ST. 10 (2007) 171-175.

[31]   B.Y. Wang, P.Z. Guo, H.Q. Bi, Q. Li, G.L. Zhang, R.Y. Wang, J.Q. Liu, X.S. Zhao, Electrocapacitive properties of $MnFe_2O_4$ electrodes in aqueous $LiNO_3$ electrolyte with surfactants, Int. J. Electrochem. Sci. 8 (2013) 8966-8977.

[32]   X.J. He, J.W. Lei, Y.J. Geng, X.Y. Zhang, M.B. Wu, M.D. Zheng, Preparation of microporous activated carbon and its electrochemical performance for electric double layer capacitor, J. Phys. Chem. Solids 70 (2009) 738-744.

[33]   Q. Cheng, J. Tang, J. Ma, H. Zhang, N. Shinya, L.C. Qin, Graphene and carbon nanotube composite electrodes for supercapacitors with ultra-high energy density, Phys. Chem. Chem. Phys. 13 (2011) 17615-17624.

[34]   S.Z. Ren, Y. Yang, M.L. Xu, H.M. Cai, C. Hao, X.Z. Wang, A new ordered mesoporous carbon with short pore length and its electrochemical performances in supercapacitor application, J. ELectrochem. Soc. 154 (2007) A731-A736.

18

[35] Q.Q. Ji, P.Z. Guo, X.S. Zhao, Preparation of chitosan-based porous carbons and their application as electrodeMaterials for supercapacitors, Acta Phys.-Chim. Sin. 26 (2010) 1254-1258.

[36] S.Z. Ren, Y. Yang, M.L. Xu, H.M. Cai, C. Hao, X.Z. Wang, Hollow SnO_2 microspheres and their carbon-coated composites for supercapacitors, Colloids Surf. A: Physicochem. Eng. Aspects 444 (2014) 26-32.

[37] J.T. Zhang, J.W. Jiang, H.L. Li, X.S. Zhao, A high-performance asymmetric supercapacitor fabricated with graphene-based electrodes, Energy Environ. Sci. 4 (2011) 4009-4015.

[38] P.L. Taberna, P. Simon, J.F. Fauvarque, Electrochemical characteristics and impedance spectroscopy studies of carbon-carbon supercapacitors, J. Electrochem. Soc. 150 (2003) A292-A300.

[39] J.S. Huang, B.G. Sumpter, V. Meunier, A universal model for nanoporous carbon supercapacitors applicable to diverse pore regimes, carbon vaterials, and electrolytes, Chem. Eur. J. 14 (2008) 6614-6626.

[40] S. Guo, Y.G. Lu, C.L. Yang, Synthesis and capacitive performances of ordered porous carbon via a template method, Chin. J. Power Sources 35 (2011) 406-408.

[41] M. Toupin, T. Brousse, D. Bélanger, Charge storage mechanism of MnO_2 electrode used in aqueous electrochemical capacitor, Chem. Mater. 16(2004) 3184-3190.

[42] K. Fic, G. Lota, E. Frackowiak, Electrochemical properties of supercapacitors

19

operating in aqueous electrolyte with surfactants, Electrochim. Acta 55 (2010) 7484-7488.

[43] L.L. Zhang, X. Zhao, M.D. Stoller, Y.W. Zhu, H.X. Ji, S. Murali, Y.P. Wu, S. Perales, B. Clevenger, R.S. Ruoff, Highly conductive and porous activated reduced graphene oxide films for high-power supercapacitors, Nano Lett. 12 (2012) 1806-1812.

[44] V. Ganesh, S. Pitchumani, V. Lakshminarayanan, New symmetric and asymmetric supercapacitors based on high surface area porous nickel and activated carbon, J. Power Sources 158 (2006) 1523-1532.

[45] X.M. Feng, Z.Z. Yan, N.N. Chen, Y. Zhang, X.F. Liu, Y.W. Ma, X.Y. Yang, W.H. Hou, Synthesis of a graphene/polyaniline/MCM-41nanocomposite and its application as a supercapacitor, New J. Chem. 37 (2013) 2203-2209.

[46] E.R. Nightingale Jr, Phenomenological theory of ion solvation: effective radii of hydrated ions, J. Phys. Chem. 63 (1959) 1381-1387.

[47] A.G. Volkov, S. Paula, D.W. Deamer, Two mechanisms of permeation of small neutral molecules and hydrated ions across phospholipid bilaye, Bioelectrochem. Bioenerg. 42 (1997) 153-160.

[48] R.B. Rakhi, W. Chen, D. Cha, H.N. Alshareef, Nanostructured ternary electrodes for energy-storage applications, Adv. Energy Mater. 3 (2012) 381-389.
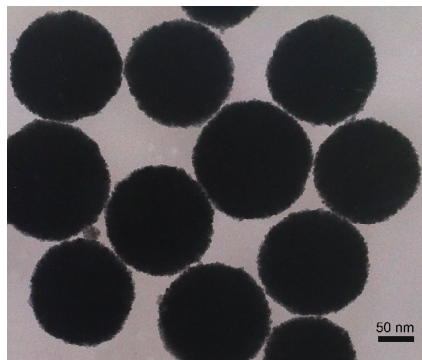
20

Figure Captions:

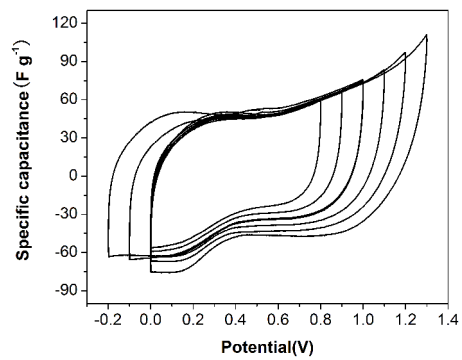**Fig. 1.** Typical TEM image of MnFe$_2$O$_4$ colloidal nanocrystal clusters.

Fig. 2. CV curves of MnFe$_2$O$_4$-based supercapacitors in aqueous 2 M KOH electrolyte under different voltage windows. Scan rate: 20 mV s^{-1}.
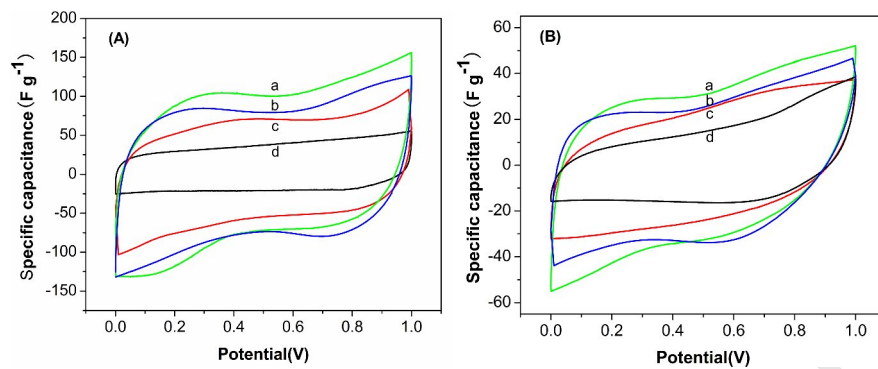
Fig. 3. CV curves of the supercapacitors with the electrolytes (2 M) of (a) KOH, (b) NaOH, (c) LiOH and (d) Na$_2$SO$_4$ at the scan rates of (A) 5 mV s^{-1} and (B) 100 mV s^{-1}.
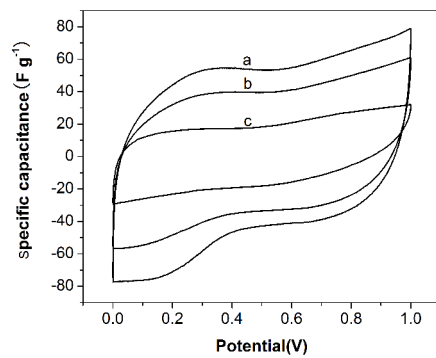
Fig. 4. CV curves of the supercapacitors with the KOH electrolytes of (a) 6 M, (b) 2 M and (c) 0.5 M at the scan rate of 50 mV s^{-1}.
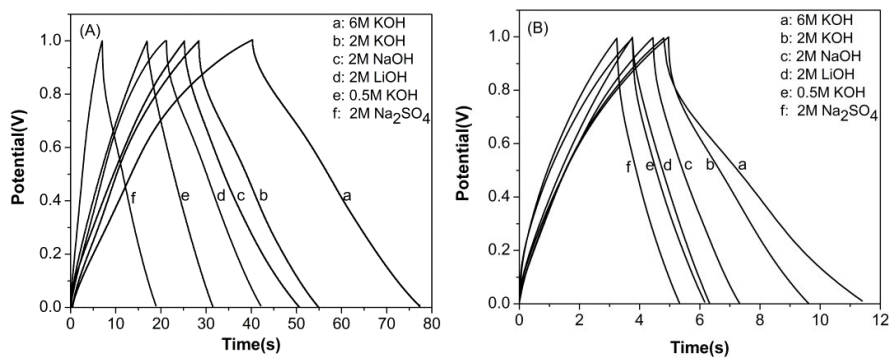
Fig. 5. Galvanostatic charge-discharge curves of MnFe$_2$O$_4$-based supercapacitors in different electrolytes at the current density of (A) 0.5 A g^{-1} and (B) 2 A g^{-1}: a: 6 M KOH, b: 2 M KOH, c: 2 M NaOH, d: 2 M LiOH, e: 0.5 M KOH, f: 2 M Na$_2$SO$_4$.
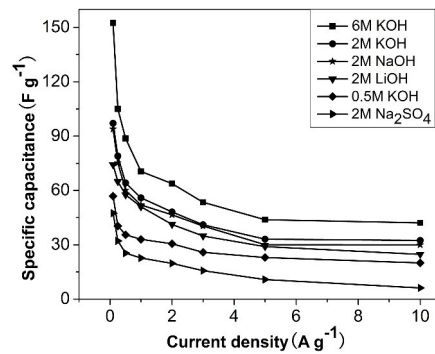
Fig. 6. Variation of the capacitances with the current density of CNCs-based supercapacitors with different electrolytes.

Fig. 7. Nyquist spectra for CNCs-based supercapacitors with aqueous (a) KOH, (b) NaOH, (c) LiOH or (d) Na$_2$SO$_4$ electrolytes.
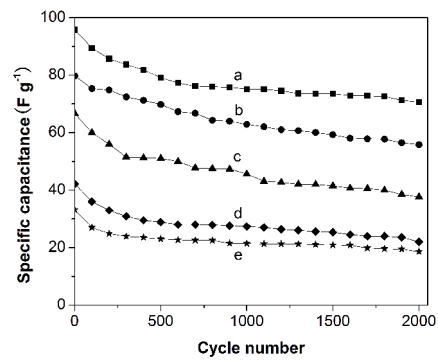
Fig. 8. Cycle stability of five types of electrolyte: a: 6 M KOH, b: 2 M KOH, c: 2 M LiOH, d: 0.5 M KOH, e: 2 M Na$_2$SO$_4$.

Scheme 1. The ion of hydrated ionic radius on the MnFe$_2$O$_4$-based supercapacitors.

21

Fig. 1. Typical TEM image of $MnFe_2O_4$ colloidal nanocrystal clusters.

22

Fig. 2. CV curves of MnFe$_2$O$_4$-based supercapacitors in aqueous 2 M KOH electrolyte under different voltage windows. Scan rate: 20 mV s^{-1}.

23

Fig. 3. CV curves of the supercapacitors with the electrolytes (2 M) of (a) KOH, (b)

NaOH, (c) LiOH and (d) Na_2SO_4 at the scan rates of (A) 5 mV s^{-1} and (B) 100 mV s^{-1}.

24

Fig. 4. CV curves of the supercapacitors with the KOH electrolytes of (a) 6 M, (b) 2

M and (c) 0.5 M at the scan rate of 50 mV s^{-1}.

25

Fig. 5. Galvanostatic charge-discharge curves of MnFe$_2$O$_4$-based supercapacitors in different electrolytes at the current density of (A) 0.5 A g^{-1} and (B) 2 A g^{-1}.

26

Fig. 6. Variation of the capacitances with the current density of CNCs-based supercapacitors with different electrolytes.
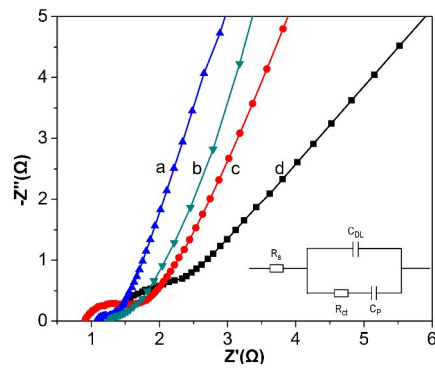
27

**Fig. 7.** Nyquist spectra for CNCs-based supercapacitors with aqueous (a) KOH, (b) NaOH, (c) LiOH or (d) Na_2SO_4 electrolytes.
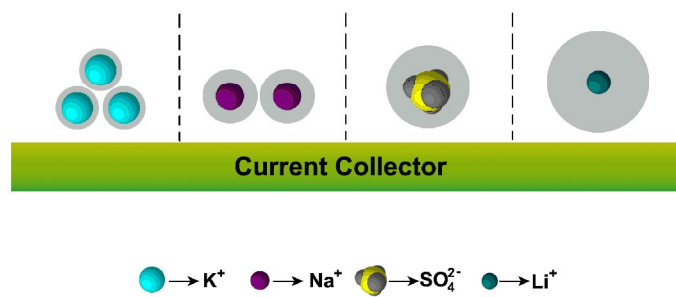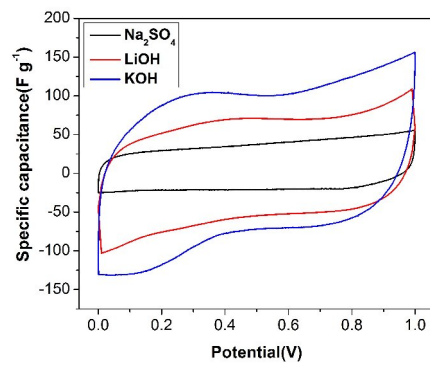
28

Fig. 8. Cycle stability of five types of electrolyte: a: 6 M KOH, b: 2 M KOH, c: 2 M

LiOH, d: 0.5 M KOH, e: 2 M Na$_2$SO$_4$.

29

Scheme 1. The ion of hydrated ionic radius on the $MnFe_2O_4$-based supercapacitors.

Graphical Abstract

31

Highlights

> The capacitance of $MnFe_2O_4$ colloidal nanocrystal clusters can be adjusted by the electrolytes.

> The assembly of colloidal nanocrystals should be important for their electrocapacitive features.

> The size of hydrated ions plays the key roles in determining the electrocapacitive features.

> The capacitance of the electrode was the largest when using the potassium hydroxide electrolyte.

32